

¹Raveendra Reddy
Enumula

²T K Ramakrishna
Rao

Development of Improved Weighed Quantum Lion Optimization with Smooth Support Vector Machine for Alzheimer's Disease



Abstract: - Accurate diagnosis of Alzheimer's disease (AD) and Mild Cognitive Impairment (MCI) was identified on an early stage is essential in the healthcare industry to stop degeneration. The Smooth Support Vector Machine (SSVM) model, Principal Component Analysis (PCA), feature extraction, and Magnetic Resonance Imaging (MRI) image preprocessing are the components for the diagnosis of AD is proposed in this research at early stage. To assist in the classifier's training, we proposed a novel Improved Weighed Quantum Lion Optimization (IWQLO). The SSVM parameters are specifically proposed to be optimized using a new Switching delayed Lion Optimization (SLO) algorithm. The IWQLO-SSVM approach was effectively used to classify AD and MCI utilizing MRI scans of the Alzheimer's disease Neuroimaging Initiative (ADNI) database and Outcome and Assessment Information Set (OASIS) database. For six example scenarios, the classification accuracy of our proposed method is acceptable. Testing show that the proposed approach improves the performance measures such as accuracy, precision, specificity, sensitivity and recall for detecting the early stage AD diagnosis.

Keywords: Alzheimer's disease, Smooth Support Vector Machine; Machine learning algorithms; Optimization technique.

I. INTRODUCTION

Models that show develops over time, i.e., the evolution of disease-related variables brain size, brain function, pathology, and cognition, are essential for reducing the severity of this highly widespread illness. By enabling critical systems like the early diagnosis of long-term cognition trajectories, systems could improve our understanding of the illness mechanisms [1]. By describing domain knowledge as statistical correlations between various components based approaches used to predict the progression of illness [2].

Pathology and healing mechanisms interact to cause AD. Together, these processes have an impact on cognition, brain function, and brain structure (including the size and activity of various brain areas) [3].

Pathology and healing mechanisms interact to cause AD. Together, these processes have an impact on cognition, brain function, and brain structure (including the size and activity of various brain areas) [3]. The demographic characteristics of a person, like their gender, level of education, hereditary susceptibility to ailment, etc., also affect to quickly an ailment develops. Therefore, it is essential to examine the brain's subregions to make an early diagnosis of AD.

Utilizing the Laplace Beltrami (LB) with Eigen value characteristic technique, computer-assisted diagnosis methods were used to analyze the volumetric variations in Corpus Callosum (CC) to detect AD early [7]. The CC was segmented using a fully automated method with the use of three modules: area assessment, template matching, and area identification. These techniques concentrated on area homogeneity, which causes inaccurate separation due to the choice of nearby pixels. Another area where there is volume loss that contributes to AD is in the CC [8].

To study the initial phases of AD, a fast cell loss is seen. Unmyelinated and myelinated neurons, correspondingly, could be seen in White Matter (WM) and Grey Matter (GM) [9–10]. Two regions of the GM are used for neuron processing and connection.

¹ *Corresponding author: Enumula, Research Scholar, Department of Computer Science and Engineering, Koneru Lakshmaiah Educational Foundation, Vaddeswaram, Guntur District, AP-522302, India.

² T K Ramakrishna Rao, Department of Computer Science and Engineering, Koneru Lakshmaiah Educational Foundation, Vaddeswaram, Guntur District, AP-522302, India.

Email- Id:¹nani.naniravi@gmail.com,²ramakrishnatk@gmail.com

Copyright © JES 2024 on-line : journal.esrgroups.org

Glial and neuronal cells, are found in WM and GM. The rest of the body parts are connected by WM aids in connecting the GM [11]. It speeds up communication between the brain and other parts, WM is also known as the "information highway" [12]. The CC splits into the right and left hemispheres with a fiber bundle called the CC. The right and left hemispheres could communicate with one another thanks to this CC [13]. The Healthy Control (HC) is a crucial part of the brain that lies beneath the medial temporal lobes; it is entirely in charge of forming new memories, retrieving existing memories is known as the "gateway of memories" [14–15]. The information must be sent to and stored in long-term memory via HC [16]. The limbic system, which contains the amygdala and HC, is reached next. Later, it permeates the entire neocortex.

AD is caused by structural modifications in the aforementioned brain regions manifest as memory loss, and issues with thinking, decision, language, and behavior. To recover the real subregions of WM, GM, CC, and HC utilizing image segmentation algorithms, research is necessary [17–19]. There are various types of image segmentation techniques, including multilayer and bilevel thresholding. Segmentation is so difficult when bi-level thresholding has a lot of problems. For two separate zones, such as the background and foreground, bi-level thresholding allows only one threshold value [20]. Multilevel thresholding approaches, on the other hand, allow for a variety of criteria to be used to divide the pixels into various groups. Bi-level thresholding's primary flaw is that it does not provide acceptable performance for actual data [21]. Therefore, multi-level thresholding was highly advised, mostly for the reasons listed above. This makes it easier to divide the histogram image into various categories.

II. RELATED WORKS

Numerous automated algorithms are available for classification such as SVM, Self Organizing Map (SOM), Neural Network (NN), and K Nearest Neighbor (KNN). These automatic classification approaches classify the data using a limited set of features derived from a variety of feature extraction methods includes Grey Level Co-occurrence Matrix (GLCM), Grey Level Run Length Matrix (GLRLM), and PCA [22–24]. Since Deep Learning (DL) approaches could perform all of these tasks within the classification stage itself used for performing operations like feature extraction and feature reduction.

Implementing a separation procedure was necessary for tracking internal brain area anatomical changes. Many image segmentation methods fall under the threshold, region, area, and other categories that mix with other theory categories [25]. A popular method for segmenting images into distinct sections is called criterion segmentation [26]. There are two categories of thresholding techniques: bi-level and multi-level thresholding. In general, bi-level thresholding methods are costly and time-consuming, whereas multilayer thresholding offers the best answer with the best threshold value and requires less computing time and a faster processing speed [27]. Therefore, switching to multilevel thresholding—also known as optimization methods and more common during the past 20 years—is necessary.

There are many advantages to using this method, including its simplicity, adaptability, and ability to discover the global optimum solution while avoiding the local optimum [28]. Although the aforementioned list of optimization strategies is driven by hunting, they won't be imitating leadership qualities. Grey Wolf Optimization (GWO) motivates hunting with its innately strong leadership traits. Convolutional Neural Network (CNN) and combinations of multiple CNN have been used to identify distinct images more accurately [29]. Due to its exceptional performance and low computational cost, the SVM has been effectively used supervised learning method to address data classification and regression issues. It should be noted that the SVM implementation's random effects choice could result in a classifier with weak resilience that the classification efficiency is highly reliant [30]. To maximize the SVM's performance, it makes sense to apply techniques to improve the SVM variables. The Kennedy and Eberhart-proposed Particle Swarm Optimization (PSO) method appear to be a viable option in the search for an appropriate method [31]. A population-based stochastic optimization technique called PSO mimics the behavior of creatures like schooling fish and flocking birds. It was demonstrated that the proposed IWQLO-SSVM classification outperforms various cutting-edge ML techniques. This paper's key contribution could be summed up as follows.

(1) Feature extraction; Image preprocessing, and the IWQLO-SSVM model constitute a novel framework for diagnoses the AD at early stage.

(2) Experiment findings show that the proposed IWQLO-SSVM classifier outperforms the other existing methods on ML techniques used to diagnose AD.

(3) Research was conducted on the sMCI and pMCI categories, which are important for early diagnosis of AD discussed in this paper.

III. SYSTEM FRAMEWORK

The National Institute on Aging (NIA), the National Institute of Biomedical Imaging and Bioengineering, Food and Drug Administration (FDA) together developed the ADNI database in the year of 2003. They specifically chose 361 participants of the ADNI baseline scans who had MRI images. An overall framework of the system is made up of MRI image preprocessing, PCA, feature extraction, PCA using IWQLO-SSVM proposed framework developed to classify the AD and MCI participants. To cope with the duplicate information in the MRI images, the image preprocessing procedures such as the ADNI registration; pipeline; separation; skull stripping, smoothing and normalization) is first applied to the MRI images shown in Figure 1. The GM tissue volumes known as the voxel characteristics are recovered from the Region of Interest (ROI) using the Automated Anatomical Labeling (AAL) template. Third, the dimension reduction step of the PCA method is utilized to streamline the data analytical method.

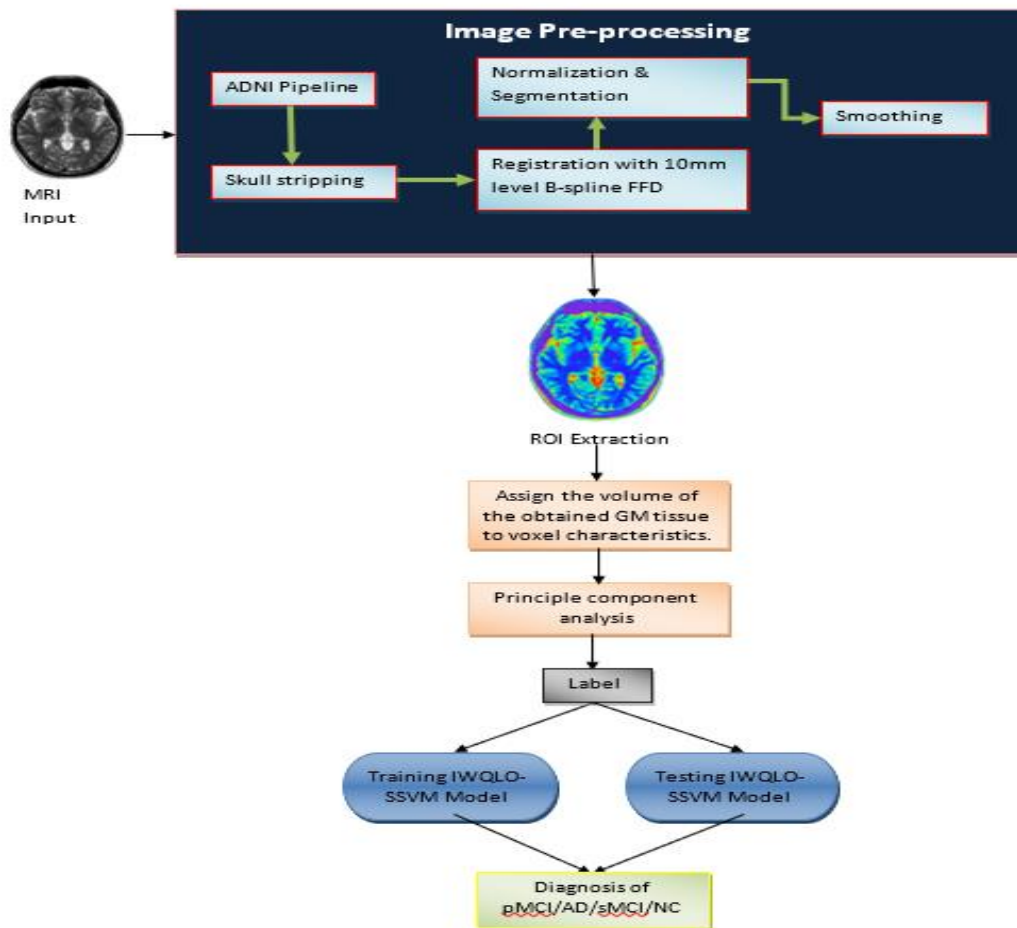


Figure 1: Proposed technique diagram

3.1 Image preprocessing

Feature extraction is carried out using a standard image preprocessing technique depends on the collected MRI images shown in Figure 2.

32490 characteristics are total, which indicates a significant computational cost. To increase computational efficiency, PCA, a dimension reduction approach that is often employed, is applied [32]. The PCA f is a linear combination of all occurrences, which reduces the amount of information.

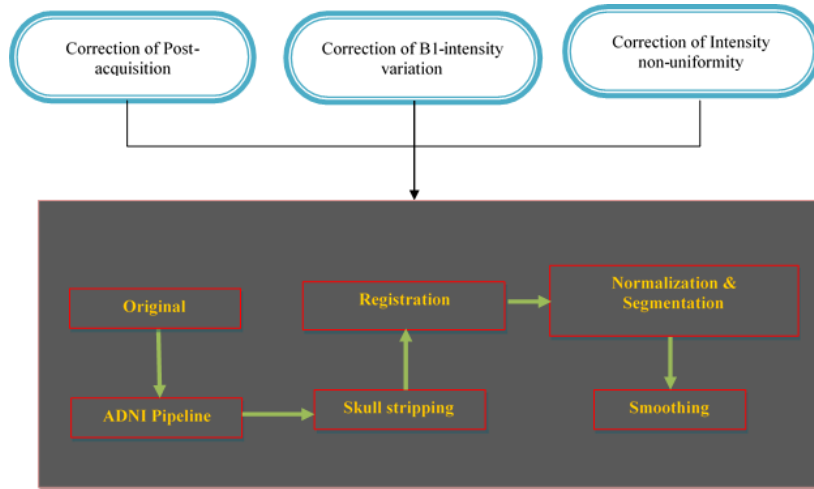


Figure 2: The preprocessing image structure

Determine X's covariance Using Equation:(1)

$$Cov = \frac{1}{n} I^T I \quad (1)$$

For the covariance Cov perform an Eigen decomposed and set the d^h largest eigenvector represented as W_d^T . The modified factors matrix F is shown in Equation:(2)

$$F = W_d^T I \quad (2)$$

Additionally, the first two principal elements' information scatters where blue vectors reflect and red dots indicate the object value within the new location.

3.2 Improved Weighed Quantum Lion Optimization

The method provided the two attributes of location P and velocity V to each particle. In iteration, the entire weighed quantum lion was subjected to the fitness function f evaluation. Two best component classifications were adjusted after each repetition. The B_p location that a component has previously reached fell into one of two categories which is shown in Equation:(3)

$$B_p(x, t) = arg \min_{h=1, \dots, t} \{f(P_x(h))\} \quad (3)$$

where x represents the index value of particle, k the iteration value of index, P is the location, t the current iteration number, and f the fitness function The second category was the best global position B_g shown in Equation:(4) using which all particles had reached up to that point:

$$B_g(t) = arg \min_{x=1, \dots, N} \{B_p(x, t)\} \quad (4)$$

where N stands for the overall particle count. The particle was updated by B_p and B_g .

$$V_x(t + 1) = w \times V_x(t) + i_p \times r_p \times (B_p(x, t) - P_x(h)) + i_g \times r_g \times (B_g(t) - P_x(t)) \quad (5)$$

$$P_x(t + 1) = P_x(t) + V_x(t + 1) \tag{6}$$

The inertia weight, shown by w in this example, helps balance regional exploitation with global exploration. The deceleration factors i_p and r_p two positive constant variables were intended to change the distances to B_p and B_g correspondingly. The random variables i_g and r_g fall between $[0, 1]$, which is shown in Equation (5), (6) & (7)

$$V_x(t + 1) \leftarrow \min(V_{max}, V_x(t + 1)) \tag{7}$$

where V_{max} is the maximum allowed particle speed.

3.3 Training proposed Algorithm

The IWQLO imitated the actions of killer lion, as a result of this, Wang and Lv presented a prey model [33] in which predators pursue the center of the bird while the prey uses a variety of escape mechanisms. Predator as y and prey are the two categories into which the swarm in IWQLO can be marked as r . In light of this concept, Equations (8), (9), (10) & (11) as follows:

$$V_x^q(t + 1) = w_q(t) \times V_x^q(t) + i_p \times r_p \times (B_p^q(x, t) - P_x^q(t)) + i_g \times r_g \times (B_g(t) - P_x^q(t)) \tag{8}$$

$$V_x^j(t + 1) = w_j(t) \times V_x^j(t) + i_p \times r_p \times (B_p^j(x, t) - P_x^j(t)) + i_g \times r_g \times (B_g(t) - P_x^j(t)) \tag{9}$$

The weight $w_q(t)$ and $w_j(t)$ are weights for IWQLO are defined as:

$$w_q(t) = 0.5 + 0.1 \times \exp\left(-\frac{10 \times t}{t_{max}}\right) \tag{10}$$

$$w_j(t) = w_{max} - t \times \frac{w_{max} - w_{min}}{t_{max}} \tag{11}$$

The rigorous statistical results were obtained using the 10-fold cross-validation. It could be applied to guarantee that the outcome was generalizable. In this configuration, one classification was produced in each trial, resulting in the creation of 10 fold cross-validation and 50 distinct independent runs of 500 different categories. Designing the ROC for each of the 500 classifications in this study would not be possible. The experiment's sensitivity, specificity, Area Under the Curve (AUC), mean, standard deviation and precision of performance measures were analyzed and evaluated in this study.

3.4 Improved Weighed Quantum Lion Optimization with Smooth Support Vector Machine (IWQLO-SSVM)

IWQLO-SSVM Algorithm steps

Input: Scanned images (MRI)

Output: Predict the AD

Step 1: Transformed into grayscale image from MRI image at axial direction $Y=61$

Step 2: Segment the Grey scale image using Wavelet Entropy at k^{th} level.

Step 3: Extract the features from segmented image

Step 4: Steps to follow SSVM features is for classifying AD

(i) Calculate the input features Using Equation: (12)

$$FE(b(n)) = \sum_{q=1}^k wei_q \delta_q(n) \quad (12)$$

(ii) Weighed Quantum estimation is performed Using Equation (13)

$$wei = (l^T l)^{-1} l^T y \quad (24)$$

(iii) RBF estimation

$$\delta_q(n) = \exp \left[\frac{-|b(n) - cen_q|^2}{2\omega_q^2} \right] \quad (14)$$

Step 5: IWQLO algorithm to calculate the optimum value using Equation (14)

Step 6: Classifies the types of AD and evaluated by the 10 fold cross validation

The proposed model, a hybrid predictor is to improve classification performance by employing IWQLO to optimize the kernel parameters and penalty factor c. The fitness function of IWQLO defined and chosen SSVM classification to improve accuracy is claculated using Equation:(15).

$$f = \frac{True\ Positive + True\ Negative}{True\ Positive + False\ Positive + False\ Negative + True\ Negative} \quad (15)$$

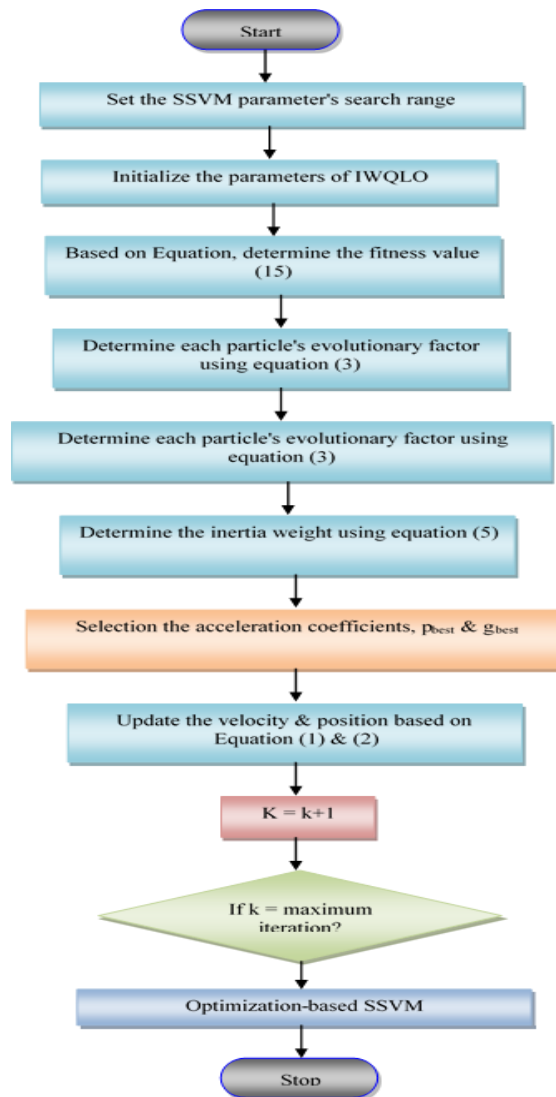


Figure 3: IWQLO-SSVM system's flowchart.

IV EXPERIMENT RESULTS

Table 1 illustrates the SSVM algorithms' classification accuracy. Table 2 shows that the proposed IWQLO-SSVM-PCA performs better when compared to the existing systems. In many instances, the IWQLO-SSVM-system without PCA can come in second. The proposed IWQLO-SSVM-PCA system outperforms the existing NC on AD and sMCI on AD diagnosis tasks. However, the effectiveness of our proposed IWQLO-SSVM-based techniques outperforms that of the SVM and other optimization methods. The proposed IWQLO-SSVM method performed better than existing SVM iterations overall. Table 2 compares the outcomes of the proposed IWQLO-SSVM-PCA system, SAE and DBN-dropout. Furthermore, the SAE approach is not used in the MCI vs. AD classification research. Table 2 demonstrates that the SDPSO-SVM-PCA approach beats both the SAE method and the DBN with dropout (74.075%).

Table 1 Classification Accuracy

Methods	SVM	Wolf Optimization-SVM	WO- SVM-PCA	IWQLO-SSVM	IWQLO-SSVM-PCA
pMCI vs sMCI	62.335	62.535	62.357	64.105	69.257
AD vs NC	78.648	79.347	82.6	79.657	82.64
sMCI vs NC	67.217	68.517	68.954	70.389	76.925
pMCI vs NC	76.932	79.689	82.657	85.257	85.257
AD vs sMCI	68.547	69.205	72.961	70.214	72.659
AD vs pMCI	52.354	54.021	55.44	54.567	58.214

Table 2: Three methods' classification performance.

Methods	IWQLO-SSVM-PCA	DBN dropout	SAE
pMCI vs sMCI	69.247	57.5	55.2
AD vs NC	82.54	92.1	86.9
sMCI vs NC	76.847	77.6	70.8
pMCI vs NC	85.324		
AD vs sMCI	72.659	70.5	N/A
AD vs pMCI	57.326		
Average	76.850	75.021	70.6

The proposed IWQLO-SSVM-PCA algorithm for the diagnosis of AD shows the improvement in the performance analysis over numerous SVM methods and other existing systems by evaluating the MRI images. Therefore, using the proposed IWQLO-SSVM-PCA model with other ML methods may produce useful outcomes. The proposed approach can be used to classify the ML systems.

4.1 Statistical Results

The hidden layer's neuron number was set to 3, and the decomposition grade was set to 4. The grid-searching method was used to find these variables. Table 3 displays the results of the 50 runs over the accuracies, particularities, and sensitivities. The proposed technique had a responsivity of 92.691.29%, a precision of 92.781.51%, a precision of 92.731.03%, and an AUC of 0.950.02 on the median across 50 runs.

Table 3: The statistical findings for our balanced dataset

Run	Sensitivity	Specificity	Accuracy
1	93.85	89.82	91.85
2	92.86	92.89	93.38
3	91.88	92.89	92.88

4	92.68	90.88	92.82
5	91.86	92.86	93.83
6	92.84	92.68	92.85
7	92.89	91.86	92.68
8	90.88	93.89	91.86
9	92.86	90.82	92.84
10	92.80	93.89	92.89
11	93.89	94.80	92.89
12	92.85	92.88	93.89
13	92.68	92.82	94.80
14	91.86	93.83	92.88
15	92.84	92.85	92.82
16	92.89	92.68	93.83
17	92.89	91.86	92.31
18	90.88	92.84	92.68
19	92.86	92.89	91.86
20	92.68	92.89	92.84
21	91.86	93.89	92.84
22	92.84	94.80	92.89
23	92.84	92.88	92.89
24	92.89	92.82	90.88
25	92.89	93.83	91.88
26	90.88	92.85	92.68
27	91.88	92.68	91.34
28	92.68	91.86	92.84
29	91.86	92.84	90.84
30	92.84	92.89	92.86
31	90.84	89.80	92.68
32	92.86	92.86	91.86
33	93.89	89.82	92.84
34	90.82	93.87	92.84
35	93.89	94.86	92.89
36	94.80	94.89	92.89
37	92.88	92.81	92.82
38	92.82	91.88	93.32
39	93.83	90.85	92.85
40	92.85	90.88	93.83
41	92.68	89.80	92.85
42	91.86	91.84	92.68
43	92.84	92.80	91.86
44	92.89	93.89	92.84
45	92.89	92.85	91.84
46	90.88	92.68	91.84
47	93.89	91.86	90.33
48	94.80	92.84	90.32
49	92.88	92.89	91.88
50	92.82	92.89	93.89
Average	±1.30	±1.52	±1.04

The ideal decomposition level was determined using the grid-searching technique. The decomposition level was reportedly set at k with an increment of 1, ranging from 1 to 8. The outcomes are displayed in Figure 3. In this experiment, the hidden layer's neuron count was adjusted from 2 to 10 with 1-point increments. Figure 4 presents the outcomes.

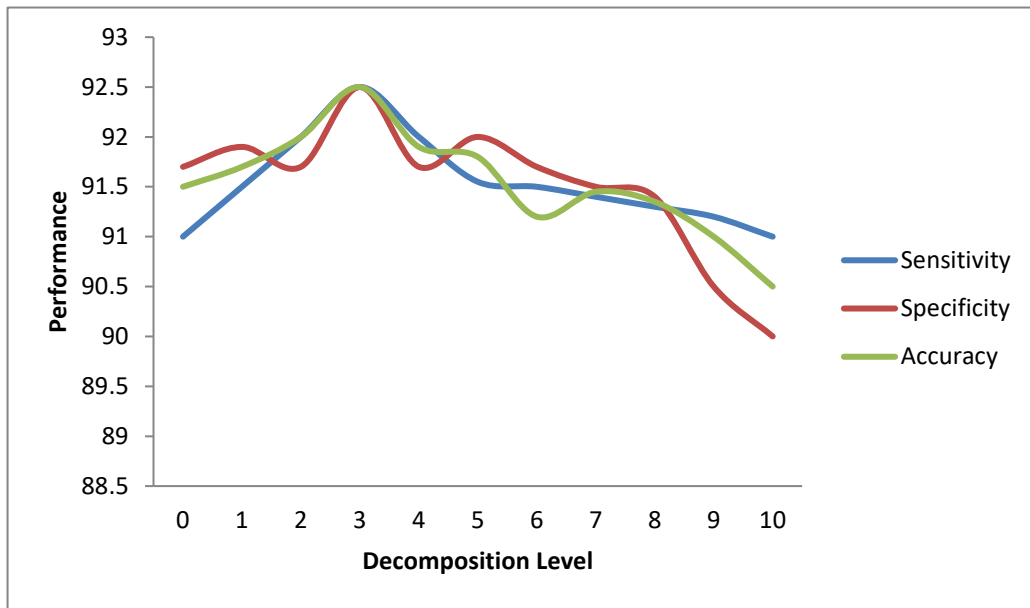


Figure 3: Optimal Decomposition Level

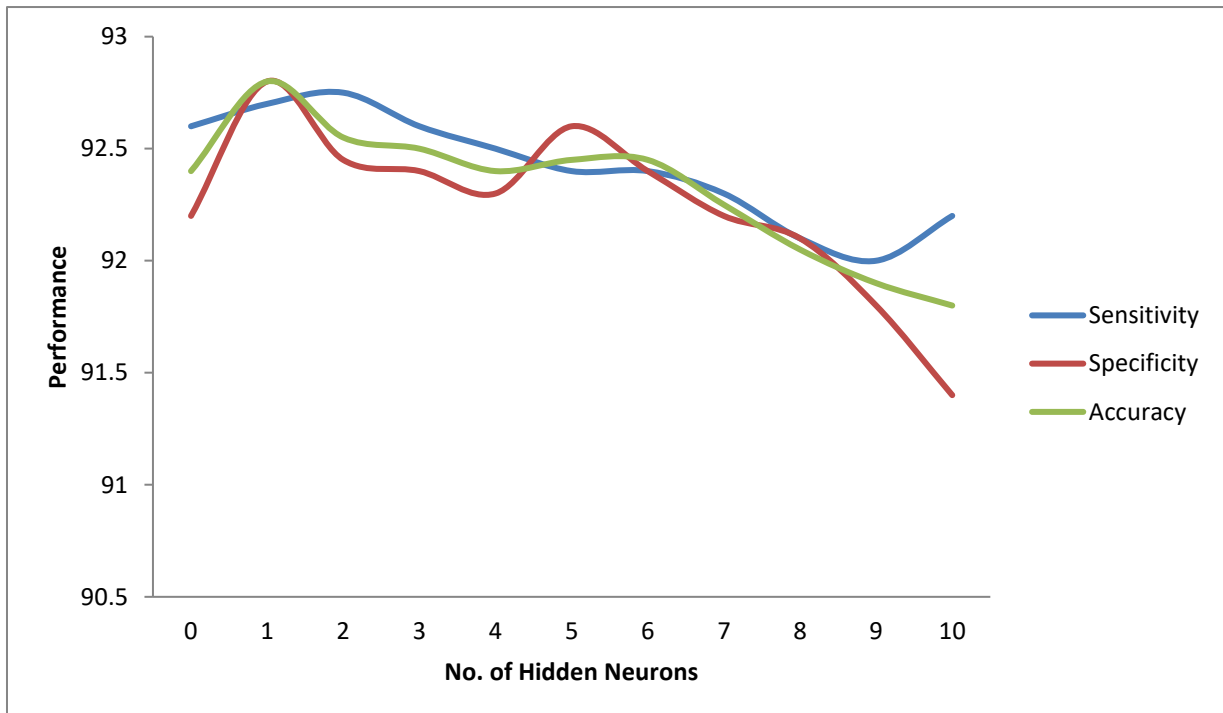


Figure 4: The ideal number of neurons in the buried layer

In the research, neither the characteristic dimension nor the neural network architecture was altered. Global optimization strategies were contrasted with the proposed IWQLO-SSVM-PCA algorithm. The maximum number of iterations was set at 1000. Each algorithm's median, quartile, whisker, and outlier were displayed using the Matlab "boxplot" function over a sample of 50 runs. The outcomes are displayed in Figure 5 (a) – (c).

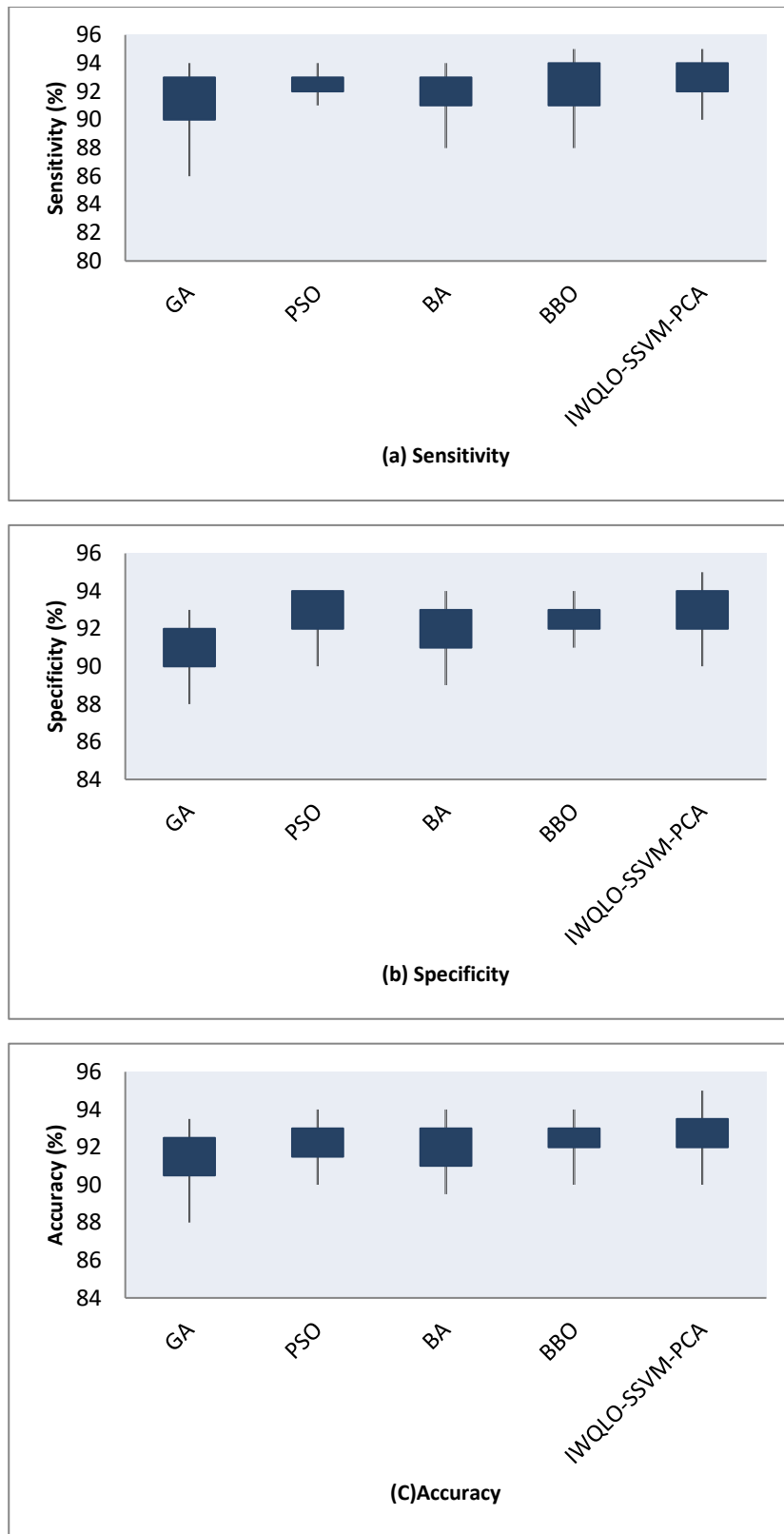


Figure 5: Comparison of training approach on proposed algorithm with existing methods based on global optimization

The proposed approach was then contrasted with established gradient-based backpropagation techniques. BP, MBP, and ABP are competing algorithms. The iteration count was set to 1000, and each algorithm was run 50 times. Figure 6 (a) – (c) displays the findings comparing the various algorithms.

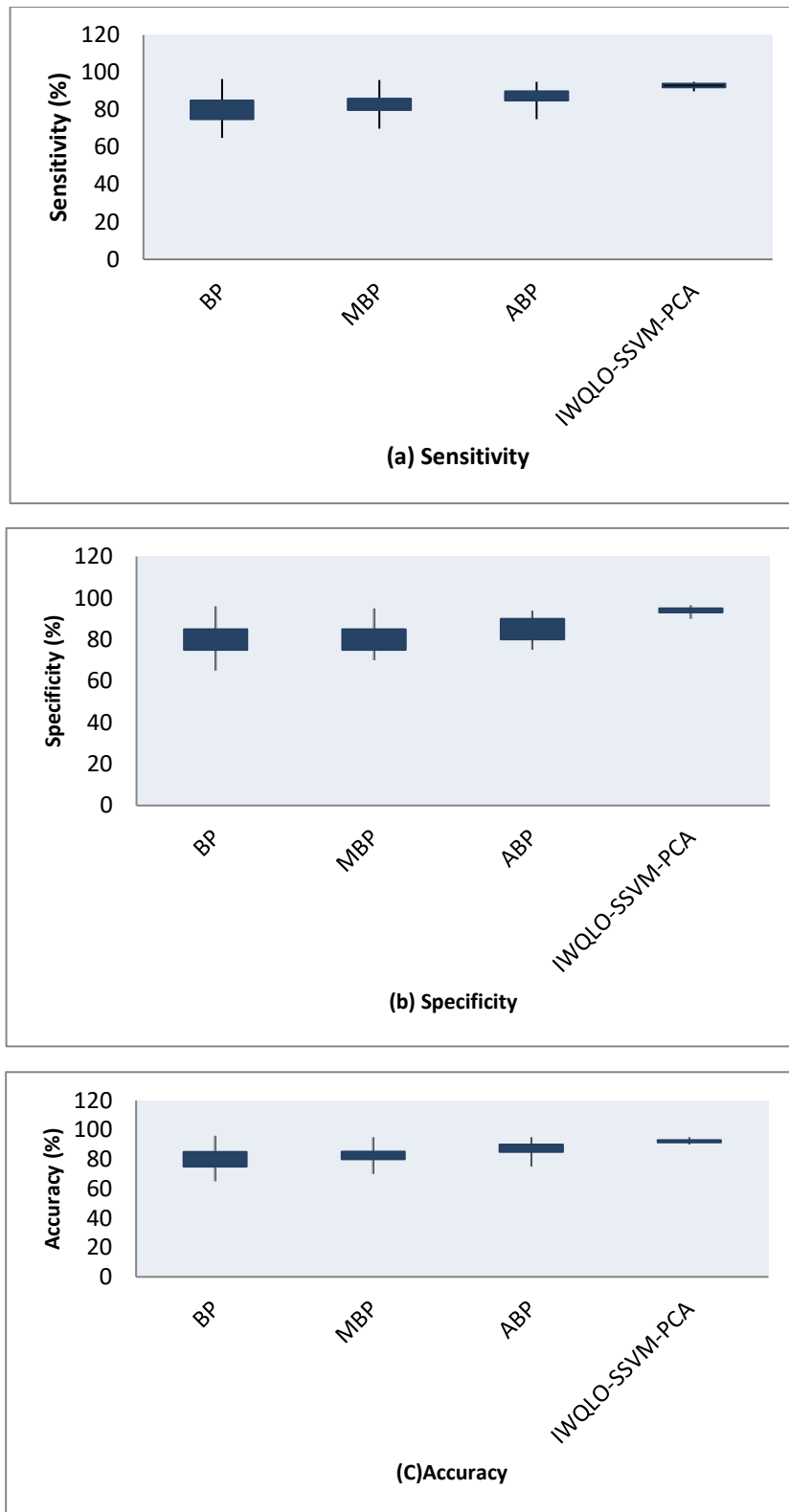


Figure 6: Comparison between our training technique and gradient-based training algorithms

4.2 Computational Complexity

Table 4 contains a list of the computation time for the offline training step. Table 5 provides the computation time for processing of image online recognition calculation time for a single volumetric image.

Table 4: The computational time required for offline training using the dataset.

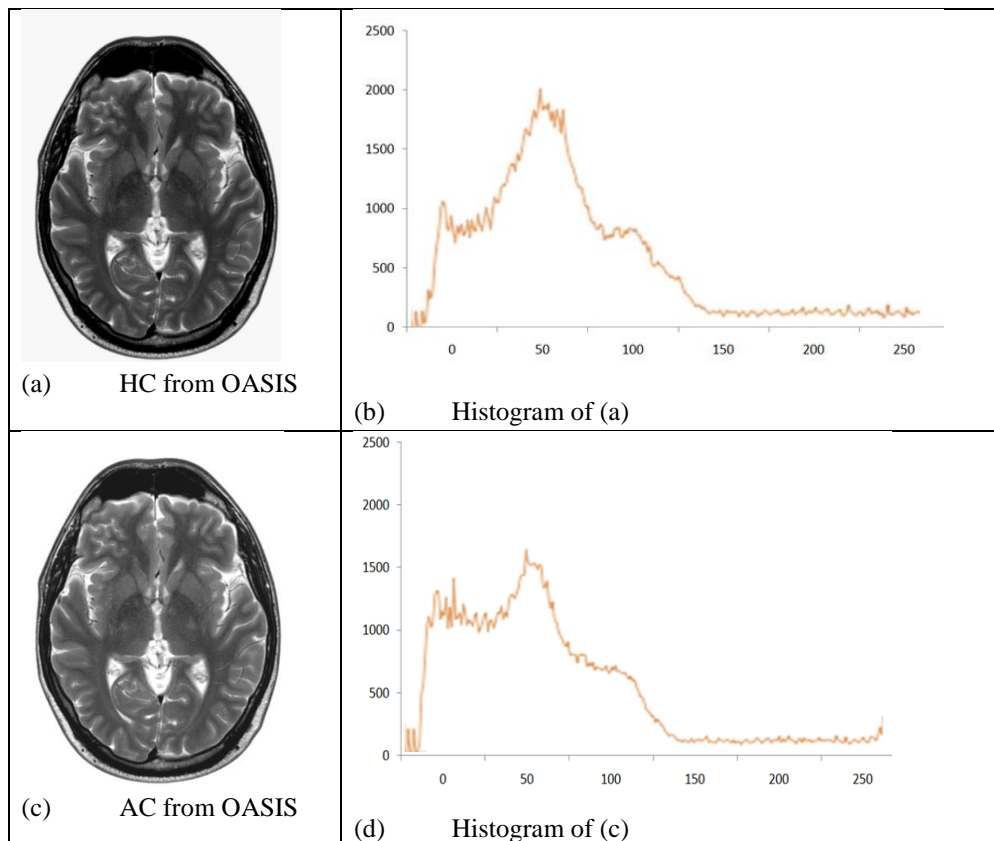
Phases	Setting	Duration
Pre-processing	199-image	41.55 hrs
Slice Selection	199-image	4.75 sec
SWE	199-image	157.32 sec
Training	50-runs	183.82 min

Table 5: Online recognition calculation time for a single volumetric image

Step	Time
Pre-processing	15.10 hrs
Slice Selection	0.03 sec
SWE	0.88 sec
Training	0.02 sec

4.3 Discussions

The identical OASIS dataset's HC and AD participants had a comparable histogram envelope, as seen in Figure 7(a–d). It is evident from Figure 7(c-f) that AD participants from nearby hospitals are higher than AD taken from OASIS. The updated histogram and smoothed version presented in Figure 7(g) display the Histogram Stretching (HS) outcome of Figure 7(e- i).



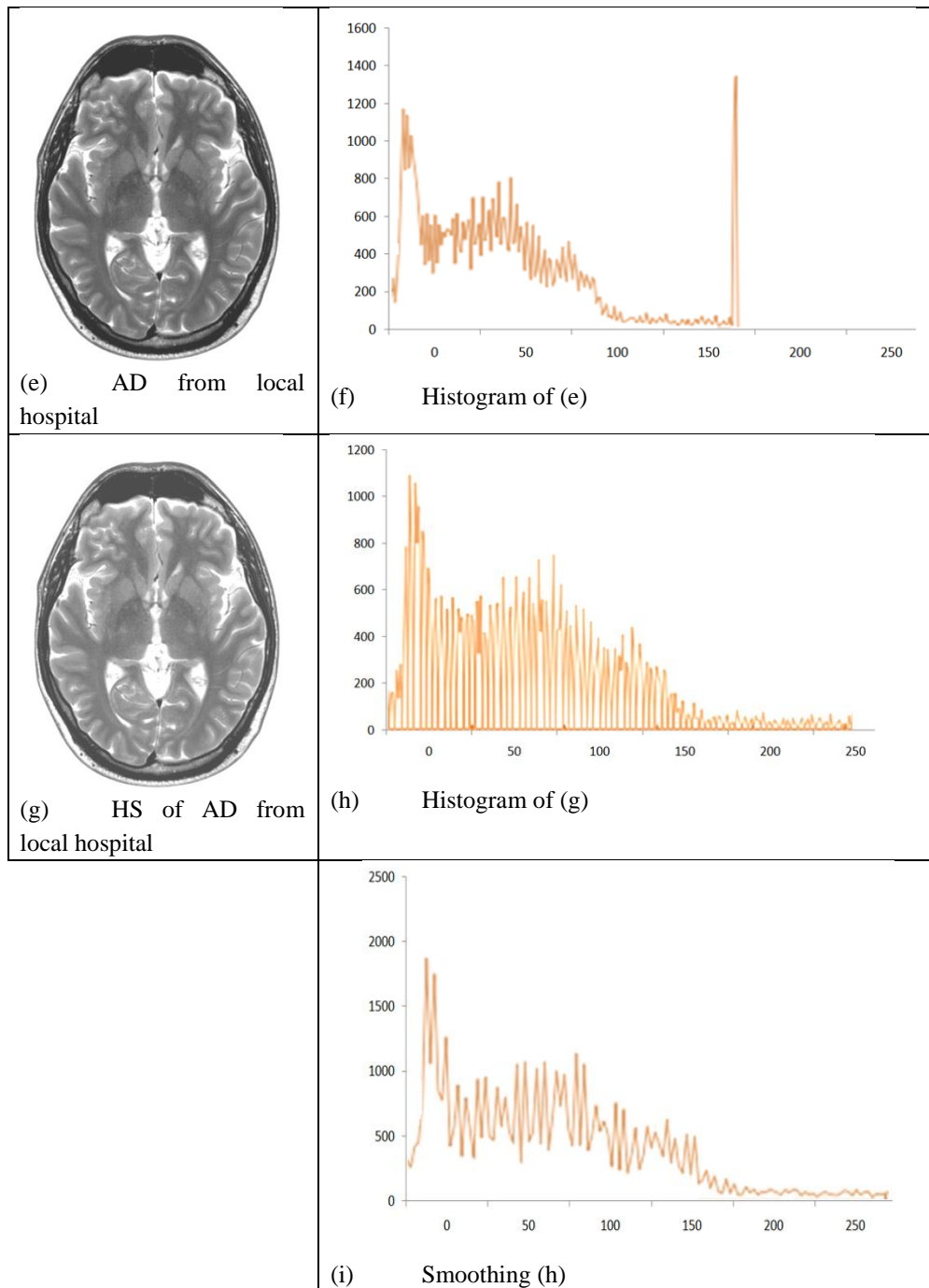


Figure 7: Histogram stretching illustration

Based on 50 runs, Table 6 displays the accuracies, specificities, and sensitivities for the balanced dataset. The algorithm used in this study demonstrated an average performance of 92.691.29% sensitivity, 92.781.51% specificity, and 92.731.03% accuracy.

The recommended IWQLO-SSVM-PCA method, which produced the maximum performance of any method, was shown to be the most reliable. The comparative results demonstrate that, in terms of sensitivity, selectivity, and accuracy, the IWQLO-SSVM-PCA had a higher mean value than the other three methods. Table 6 illustrates that while the precision of the three human observers is between 72% and 78% that of the optimization technique is 91.94%. This again demonstrates the power of machine learning and computer vision.

Table 6: Manual interpretation comparison

	Sensitivity	Specificity	Accuracy
Observer 1	74.92	79.52	78.44
Observer 2	69.58	74.37	73.85
Observer 3	79.58	71.82	74.21
Proposed Algorithm	91.32	92.33	91.95

V. CONCLUSION

Our group created a revolutionary technology based on machine learning and computer vision. To assist in training the classifier, they proposed a brand-new predator-prey particle swarm optimization and created a new IWQLO-SSVM technique. For the diagnosis of AD, in particular, image pretreatment, feature extraction, PCA, and classification using the IWQLO-SSVM method are carried out. The newly developed system of the IWQLO-SSVM-PCA model outperforms two other cutting-edge deep learning techniques and multiple SVM algorithms. When the OASIS database and the information from neighborhood clinics are merged, the proposed system outperforms ten other cutting-edge methods. Additionally, the proposed system performs better than human observers in the analysis of accurate brain imaging data. We'll strive to identify minor cognitive impairment in the future. Additionally, we'll conduct preliminary experiments utilizing sophisticated classifiers like CNN or autoencoders.

References

- [1] Lee, S., Kim, J., Kang, H., Kang, D. Y., & Park, J. (2021). Genetic algorithm based deep learning neural network structure and hyperparameter optimization. *Applied Sciences*, 11(2), 744.
- [2] Ezzati, A., Harvey, D. J., Habeck, C., Golzar, A., Qureshi, I. A., Zammit, A. R., ... & Alzheimer's Disease Neuroimaging Initiative. (2020). Predicting amyloid- β levels in amnesic mild cognitive impairment using machine learning techniques. *Journal of Alzheimer's Disease*, 73(3), 1211-1219.
- [3] Grueso, S., & Viejo-Sobera, R. (2021). Machine learning methods for predicting progression from mild cognitive impairment to Alzheimer's disease dementia: a systematic review. *Alzheimer's Research & Therapy*, 13(1), 1-29.
- [4] Ezzati, A., Lipton, R. B., & Alzheimer's Disease Neuroimaging Initiative. (2020). Machine learning predictive models can improve efficacy of clinical trials for Alzheimer's disease. *Journal of Alzheimer's Disease*, 74(1), 55-63.
- [5] Arco, J. E., Ramírez, J., Górriz, J. M., Ruz, M., & Alzheimer's Disease Neuroimaging Initiative. (2021). Data fusion based on searchlight analysis for the prediction of Alzheimer's disease. *Expert Systems with Applications*, 185, 115549.
- [6] Shi, Y., Wang, Z., Chen, P., Cheng, P., Zhao, K., Zhang, H., ... & Alzheimer's Disease Neuroimaging Initiative. (2020). Episodic Memory-Related Imaging Features as Valuable Biomarkers for the Diagnosis of Alzheimer's Disease: A Multicenter Study Based on Machine Learning. *Biological Psychiatry: Cognitive Neuroscience and Neuroimaging*.
- [7] Ge, X. Y., Cui, K., Liu, L., Qin, Y., Cui, J., Han, H. J., ... & Yu, H. M. (2021). Screening and predicting progression from high-risk mild cognitive impairment to Alzheimer's disease. *Scientific Reports*, 11(1), 1-10.
- [8] Shojaie, M., Tabarestani, S., Cabrerizo, M., DeKosky, S. T., Vaillancourt, D. E., Loewenstein, D., ... & Adjouadi, M. (2021). Pet imaging of tau pathology and amyloid- β , and mri for alzheimer's disease feature fusion and multimodal classification. *Journal of Alzheimer's disease*, 84(4), 1497-1514.
- [9] Silva-Spínola, A., Baldeiras, I., Arrais, J. P., & Santana, I. (2022). The road to personalized medicine in Alzheimer's disease: The use of artificial intelligence. *Biomedicine*, 10(2), 315.
- [10] Das, S., Panigrahi, P., & Chakrabarti, S. (2021). Corpus Callosum Atrophy in Detection of Mild and Moderate Alzheimer's Disease Using Brain Magnetic Resonance Image Processing and Machine Learning Techniques. *Journal of Alzheimer's disease reports*, 5(1), 771.
- [11] Beacher, F. D., Mujica-Parodi, L. R., Gupta, S., & Ancora, L. A. (2021). Machine Learning Predicts Outcomes of Phase III Clinical Trials for Prostate Cancer. *Algorithms*, 14(5), 147.
- [12] T. P. Latchoumi, R. Swathi, P. Vidyasri and K. Balamurugan, "Develop New Algorithm To Improve Safety On WMSN In Health Disease Monitoring," *2022 International Mobile and Embedded Technology Conference (MECON)*, 2022, pp. 357-362, doi: 10.1109/MECON53876.2022.9752178.

- [13] Vélez, J. I., Samper, L. A., Arcos-Holzinger, M., Espinosa, L. G., Isaza-Ruget, M. A., Lopera, F., & Arcos-Burgos, M. (2021). A Comprehensive Machine Learning Framework for the Exact Prediction of the Age of Onset in Familial and Sporadic Alzheimer's Disease. *Diagnostics*, 11(5), 887.
- [14] Sarica, A. (2022). Editorial for the special issue on "Machine Learning in Healthcare and Biomedical Application". *Algorithms*, 15(3), 97.
- [15] Estevez, M., Benedum, C. M., Jiang, C., Cohen, A. B., Phadke, S., Sarkar, S., & Bozkurt, S. (2022). Considerations for the Use of Machine Learning Extracted Real-World Data to Support Evidence Generation: A Research-Centric Evaluation Framework. *Cancers*, 14(13), 3063.
- [16] Ekong, F., Yu, Y., Patamia, R. A., Feng, X., Tang, Q., Mazumder, P., & Cai, J. (2022). Bayesian Depth-Wise Convolutional Neural Network Design for Brain Tumor MRI Classification. *Diagnostics*, 12(7), 1657.
- [17] Van Dyk, K., Ahn, J., Zhou, X., Zhai, W., Ahles, T. A., Bethea, T. N., ... & Root, J. C. (2022). Associating persistent self-reported cognitive decline with neurocognitive decline in older breast cancer survivors using machine learning: The Thinking and Living with Cancer study. *Journal of Geriatric Oncology*.
- [18] Latchoumi, T. P., Balamurugan, K., Dinesh, K., & Ezhilarasi, T. P. (2019). Particle swarm optimization approach for waterjet cavitation peening. *Measurement*, 141, 184-189.
- [19] Haneef, R., Tijhuis, M., Thiébaud, R., Májek, O., Pristaš, I., Tolenan, H., & Gallay, A. (2022). Methodological guidelines to estimate population-based health indicators using linked data and/or machine learning techniques. *Archives of Public Health*, 80(1), 1-12.
- [20] Chen, D., Yi, F., Qin, Y., Zhang, J., Ge, X., Han, H., ... & Alzheimer's Disease Neuroimaging Initiative. (2022). A Stacking Framework for Multi-Classification of Alzheimer's Disease Using Neuroimaging and Clinical Features. *Journal of Alzheimer's Disease*, (Preprint), 1-10.
- [21] Vargas-Hakim, G. A., Mezura-Montes, E., & Acosta-Mesa, H. G. (2021). A review on convolutional neural network encodings for neuroevolution. *IEEE Transactions on Evolutionary Computation*, 26(1), 12-27.
- [22] Yu, Y., Rashidi, M., Samali, B., Mohammadi, M., Nguyen, T. N., & Zhou, X. (2022). Crack detection of concrete structures using deep convolutional neural networks optimized by enhanced chicken swarm algorithm. *Structural Health Monitoring*, 147592172111053546.
- [23] Al-Andoli, M. N., Tan, S. C., Cheah, W. P., & Tan, S. Y. (2021). A review on community detection in large complex networks from conventional to deep learning methods: a call for the use of parallel meta-heuristic algorithms. *IEEE Access*, 9, 96501-96527.
- [24] He, C., Li, X., Liu, Y., Yang, B., Wu, Z., Tan, S., ... & Weng, H. (2022). Combining multicolor fluorescence imaging with multispectral reflectance imaging for rapid citrus Huanglongbing detection based on lightweight convolutional neural network using a handheld device. *Computers and Electronics in Agriculture*, 194, 106808.
- [25] Nasser Al-Andoli, M., Chiang Tan, S., & Ping Cheah, W. (2022). Distributed parallel deep learning with a hybrid backpropagation-particle swarm optimization for community detection in large complex networks.
- [26] Baghdadi, N. A., Malki, A., Balaha, H. M., Badawy, M., & Elhosseini, M. (2022). A3C-TL-GTO: Alzheimer Automatic Accurate Classification Using Transfer Learning and Artificial Gorilla Troops Optimizer. *Sensors*, 22(11), 4250.
- [27] Al-Andoli, M. N., Tan, S. C., & Cheah, W. P. (2022). Distributed parallel deep learning with a hybrid backpropagation-particle swarm optimization for community detection in large complex networks. *Information Sciences*, 600, 94-117.
- [28] Thavasimani, K., & Srinath, N. K. (2022). Hyperparameter optimization using custom genetic algorithm for classification of benign and malicious traffic on internet of things-23 dataset. *International Journal of Electrical & Computer Engineering (2088-8708)*, 12(4).
- [29] Asgari Taghanaki, S., Abhishek, K., Cohen, J. P., Cohen-Adad, J., & Hamarneh, G. (2021). Deep semantic segmentation of natural and medical images: a review. *Artificial Intelligence Review*, 54(1), 137-178.
- [30] Wang, Z., Wang, E., & Zhu, Y. (2020). Image segmentation evaluation: a survey of methods. *Artificial Intelligence Review*, 53(8), 5637-5674.
- [31] Mehmood, A., Maqsood, M., Bashir, M., & Shuyuan, Y. (2020). A deep Siamese convolution neural network for multi-class classification of Alzheimer disease. *Brain sciences*, 10(2), 84.
- [32] Ezzati, A., Zammit, A. R., Harvey, D. J., Habeck, C., Hall, C. B., Lipton, R. B., & Alzheimer's Disease Neuroimaging Initiative. (2019). Optimizing machine learning methods to improve predictive models of Alzheimer's disease. *Journal of Alzheimer's Disease*, 71(3), 1027-1036.